

# Time dependent nucleation. II. A semiclassical approach

Lucio Demeio and Bernie Shizgal<sup>a)</sup>

*Department of Chemistry, University of British Columbia, Vancouver, British Columbia, Canada V6T 1Z1*

(Received 28 October 1992; accepted 2 December 1992)

The continuum approximation of the Becker–Döring birth and death equations [B. Shizgal and J. C. Barrett, *J. Chem. Phys.* **91**, 6505 (1989)] leads to a Fokker–Planck equation for the continuous cluster distribution. This linear Fokker–Planck equation is solved with the expansion of the cluster distribution function in the eigenfunctions of the Fokker–Planck operator. The Fokker–Planck eigenvalue problem can be transformed into an equivalent Schrödinger equation. In this paper, the semiclassical Wentzel–Kramers–Brillouin (WKB) method and the corresponding supersymmetric WKB method are employed in the determination of the eigenvalues and eigenfunctions of the equivalent Schrödinger equation. We compare the approximate results with those obtained with a standard discretization scheme. We obtain eigenvalues and eigenfunctions of the Fokker–Planck operator which are in good agreement with the exact ones. The nucleation fluxes and associated time lags are also considered.

## I. INTRODUCTION

Homogeneous nucleation is the process by which clusters of a new phase are generated from a parent phase. It occurs when the saturation ratio of a vapor is suddenly increased above a certain critical value. After a transient period, characterized by a time lag  $\tau$ , the cluster concentration and the nucleation flux reach steady-state values corresponding to the new saturation ratio. This phenomenon has been studied for many years, and various models, which give very different predictions for the nucleation fluxes and time lags, have been developed.<sup>1–11</sup>

Classical nucleation theory is based on the discrete cluster size distribution given by the Becker–Döring birth and death equations.<sup>1</sup> The steady-state nucleation rate is determined with the introduction of a continuum approximation to the discrete birth and death equations as considered by Frenkel<sup>2</sup> and later by Goodrich.<sup>3</sup> Shizgal and Barrett<sup>4</sup> (referred to as I) examined the transformation of the discrete birth and death equations to a continuous Fokker–Planck equation for the continuous cluster distribution and compared this approach with the formalism of Frenkel and Goodrich. Wu<sup>5</sup> has very recently examined this different formulation and concluded that the approach by Shizgal and Barrett is indeed more accurate than the previous approaches.

Shizgal and Barrett also considered the transformation of the Fokker–Planck equation (associated with the time-dependent nucleation) to a Schrödinger equation. The eigenvalues of the Fokker–Planck operator are then interpreted as the energy levels of a potential function in the corresponding Schrödinger equation. The main purpose of the present paper is to employ the Wentzel–Kramers–Brillouin<sup>12</sup> (WKB) and supersymmetric<sup>13</sup> WKB (SWKB)

methods in the approximate solution of the eigenvalue problem and the time dependent cluster distribution function.

The continuum approach has been used previously. Kashiev<sup>6</sup> expands the solution in the eigenfunctions of an equivalent Schrödinger eigenvalue problem and approximates the corresponding Schrödinger potential with a square well potential. As discussed by Shizgal and Barrett<sup>4</sup> and as shown in the present work, this approximation is valid only in the vicinity of the critical cluster. A similar approach is adopted by Binder and Stauffer,<sup>7</sup> who derive the differential equation for the cluster distribution function from a general master-equation description and obtain an estimate for the time lag based on a variational principle. Trinkaus and Yoo<sup>8</sup> solve the Fokker–Planck equation with the aid of the Green's function approach. Also, Edrei and Gitterman<sup>9</sup> and Rabin and Gitterman<sup>10</sup> solve the Fokker–Planck equation by replacing the actual potential with that of the harmonic oscillator and modifying the lower boundary condition so that the solution can be expanded in the eigenfunctions of the harmonic oscillator. Their diffusion coefficient, however, has a different functional dependence on cluster size than the one considered by the other workers and in the present paper. Shi, Seinfeld, and Okuyama<sup>11</sup> adopt a singular perturbation approach to obtain approximate solutions of the Fokker–Planck equation that describes the transient nucleation process in liquid systems.

In this paper, we do not provide a detailed comparison of the various models and their predictions, but rather show how the WKB and SWKB approximations can be employed to solve the equations that arise in one particular model and compare the values obtained for the nucleation fluxes and time lags with the exact ones. We use the approach by Frenkel although it does not give the most accurate results. However, for this model the poten-

<sup>a)</sup>Also with the Department of Geophysics and Astronomy.

tial in the Schrödinger equation is analytic<sup>4</sup> and the application of the WKB and SWKB methods is simplified. We anticipate that the results obtained for the other choices of Fokker–Planck equations would be similar to those obtained in this paper. We apply our method to the case of vapor condensation of water.

## II. THEORY

The main quantity of interest is the cluster distribution  $f_i(t)$ , which represents the number of clusters of size  $i$  that contain  $i$  monomers. The time evolution of  $f_i(t)$  is governed by the birth and death equations introduced by Becker and Döring,<sup>1</sup> whose solution has been discussed elsewhere.<sup>4</sup> With the assumption that the size of a cluster can vary only by the gain or loss of a single monomer, the birth and death equations are of the form

$$\frac{df_i(t)}{dt} = J_{i-1}(t) - J_i(t), \quad (1)$$

where the nucleation flux  $J_i(t)$  is defined by

$$J_i(t) = \beta_i f_i(t) - \alpha_{i+1} f_{i+1}(t) \quad (2)$$

and gives the number per unit time of clusters of size  $i$  which become clusters of size  $i+1$ . Here,  $\alpha_i$  and  $\beta_i$  are the rate coefficients for the loss and the gain of a monomer by a cluster of size  $i$ . Rigorous expressions for the rate coefficients, determined from first principles in the framework of a classical or quantum treatment of the elementary reactions, do not exist in the literature and it is therefore customary to assume empirical formulas for them. A typical choice is

$$\beta_i = S b i^{2/3}, \quad (3)$$

where  $S = P/P_e$  is the saturation parameter,  $P$  the vapor pressure,  $P_e$  the equilibrium vapor pressure of the liquid at temperature  $T$ , and  $b = A_c P_e / \sqrt{2\pi m k T}$ , with  $m$  and  $A_c$  the monomer mass and surface area, respectively. The principle of detailed balance at equilibrium then gives<sup>4</sup>

$$\alpha_i = b(i-1)^{2/3} \exp[A_c \sigma (i^{2/3} - (i-1)^{2/3})], \quad (4)$$

where  $\sigma$  is the bulk surface tension.

In classical nucleation theory, the birth and death equations (1) are usually replaced by a Fokker–Planck-type differential equation. Namely, one introduces a continuous variable  $x$  instead of the discrete cluster size  $i$  and the cluster distribution then becomes  $f(x,t)$ . Analogously, the continuous rate coefficients are  $\alpha(x)$  and  $\beta(x)$ . As discussed in I, there are many ways of going from the discrete birth and death equations for  $f_i(t)$  to a continuous differential equation for  $f(x,t)$ . The Fokker–Planck equation for  $f(x,t)$  is of the form

$$\frac{\partial f}{\partial t} = \frac{\partial}{\partial x} [A(x)f(x,t)] + \frac{\partial^2}{\partial x^2} [B(x)f(x,t)], \quad (5)$$

and the drift and diffusion coefficients  $A(x)$  and  $B(x)$  depend on the details of the transformation from the discrete equations to their continuous limit. Independently of the particular transformation considered, however, we have

$$A(x) = B(x) \frac{\phi'(x)}{kT} - B'(x), \quad (6)$$

where

$$\phi(x) = A_c \sigma (x^{2/3} - 1) - (x-1)kT \ln S \quad (7)$$

is the free energy in the supersaturated vapor. Also, the continuous form of the nucleation flux (2) is

$$J(x,t) = - \left[ A(x)f(x,t) + \frac{\partial}{\partial x} B(x)f(x,t) \right]. \quad (8)$$

The equilibrium solution of Eq. (5), corresponding to  $J(x,t) \equiv 0$ , is

$$f^{\text{eq}}(x) = f^{\text{eq}}(1) \frac{B(1)}{B(x)} \exp \left[ - \int_1^x \frac{A(x')}{B(x')} dx' \right]. \quad (9)$$

With  $A(x)$  given by Eq. (6), we have

$$f^{\text{eq}}(x) = f^{\text{eq}}(1) \exp \left[ - \frac{\phi(x)}{kT} \right]. \quad (10)$$

With the definition  $F(x,t) = f(x,t)/f^{\text{eq}}(x)$ , the Fokker–Planck equation becomes

$$\begin{aligned} \frac{\partial F}{\partial t} = LF &\equiv -A(x) \frac{\partial F}{\partial x} + B(x) \frac{\partial^2 F}{\partial x^2} \\ &= \frac{1}{f^{\text{eq}}(x)} \frac{\partial}{\partial x} \left[ B(x)f^{\text{eq}}(x) \frac{\partial F}{\partial x} \right]. \end{aligned} \quad (11)$$

The boundary conditions for the Fokker–Planck equation follow from the assumption that the amount of monomers in the system remains constant and equal to the equilibrium value and that there are no clusters of size greater than a cutoff value  $N$ . We then have

$$\begin{aligned} F(1,t) &= 1, \\ F(x,t) &= 0, \quad x > N. \end{aligned} \quad (12)$$

Because of these boundary conditions, the Fokker–Planck equation has a steady-state solution  $F^{\text{SS}}(x)$ , corresponding to a steady flux  $J(x,t) = J^{\text{SS}}$ . It is easily seen that the steady flux and the steady distribution are given by,

$$J^{\text{SS}} = \left[ \int_1^N \frac{dx'}{B(x')f^{\text{eq}}(x')} \right]^{-1}, \quad (13)$$

$$F^{\text{SS}}(x) = J^{\text{SS}} \int_1^N \frac{dx'}{B(x')f^{\text{eq}}(x')}. \quad (14)$$

An important quantity in nucleation theory is the critical cluster size  $x^*$ , which corresponds to the maximum of the free energy  $\phi(x)$ . This is the cluster size at which the surface contribution and the bulk contribution to the free energy are equal. The surface contribution, proportional to the cluster surface area, favors cluster growth, while the bulk contribution, proportional to the cluster volume,

tends to oppose it. Therefore, clusters bigger than  $x^*$  grow in time, while clusters smaller than  $x^*$  decrease their size with time. From Eq. (7), we have that

$$x^* = \left( \frac{2A_c\sigma}{3kT \ln S} \right)^3. \quad (15)$$

The equilibrium distribution  $f^{eq}(x)$  will be sharply peaked at  $x=x^*$ . If  $\phi(x)$  is expanded to second order about  $x=x^*$ , the nucleation flux and the steady distribution are given by

$$j^{SS} = B(x^*) f^{eq}(x^*) \left[ -\frac{\phi''(x^*)}{2\pi kT} \right]^{1/2}, \quad (16)$$

$$F^{SS}(x) = \frac{1}{2} \left( 1 + \operatorname{erf} \left[ \left[ -\frac{\phi''(x^*)}{2kT} \right]^{1/2} (x-x^*) \right] \right), \quad (17)$$

where  $\operatorname{erf}(x)$  is the error function. In Ref. 4 three different transformations from the discrete equations to the Fokker-Planck equation were considered and the solutions of the Fokker-Planck equations were compared with the solutions of the birth and death equations. Since the present work focuses on the WKB (and SWKB) approximation to the solution of the Fokker-Planck equation (11), we shall specifically consider only one of these transformations, namely the one given by Frenkel.<sup>12</sup> Wu<sup>5</sup> has recently presented a detailed analysis of these three different transformations to a continuous cluster distribution function.

With the Frenkel form of the Fokker-Planck equation, we have for the diffusion coefficient,

$$B(x) = \beta(x) = Sbx^{2/3}. \quad (18)$$

Furthermore, it is convenient to introduce the function  $\hat{F} \equiv [F(x,t) - F^{SS}(x,t)](f^{eq})^{1/2}(x)$ . The Fokker-Planck equation can then be written as

$$\frac{\partial \hat{F}}{\partial t} = -\hat{L}\hat{F}, \quad (19)$$

where the operator  $\hat{L}$  is given by  $\hat{L} = (f^{eq})^{1/2} L (f^{eq})^{-1/2}$ . Then, the solution of the Fokker-Planck equation can be written as

$$F(x,t) = F^{SS}(x,t) + \frac{1}{(f^{eq})^{1/2}} \sum_n c_n \psi_n(x) e^{-\lambda_n t} \quad (20)$$

with  $\lambda_n$  and  $\psi_n(x)$  the eigenvalues and eigenfunctions of  $\hat{L}$ , that is,

$$\hat{L}\psi_n(x) = \lambda_n \psi_n(x). \quad (21)$$

The boundary conditions are  $\psi_n(1) = \psi_n(N) = 0$  and the  $c_n$ 's are the expansion coefficients of the initial distribution, given by

$$c_n = \int_1^N dx [F(x,0) - F^{SS}(x)] (f^{eq})^{1/2}(x) \psi_n(x). \quad (22)$$

The initial distribution is usually of the form

$$F(x,0) = \begin{cases} F^{SS}(x), & x \leq x_0 \\ 0, & x > x_0 \end{cases} \quad (23)$$

in which case Eq. (22) becomes

$$c_n = - \int_{x_0}^N dx F^{SS}(x) (f^{eq})^{1/2}(x) \psi_n(x). \quad (24)$$

With the further transformation<sup>14-16</sup>

$$y = \int_1^x \frac{dx'}{\sqrt{B(x')}}, \quad (25)$$

$$\chi_n(y) = [B(x)]^{1/4} \psi_n(x), \quad (26)$$

the eigenvalue equation (21) for  $\hat{L}$  can be transformed into a Schrödinger eigenvalue problem,

$$\chi_n''(y) + [\lambda_n - V(y)] \chi_n(y) = 0. \quad (27)$$

The Schrödinger potential  $V(y)$  is of the form of the potentials that occur in supersymmetric quantum mechanics,<sup>13,16</sup> that is,

$$V(y) = W^2(y) - W'(y), \quad (28)$$

where  $W(y)$  is the superpotential and in this case is given by

$$W(y) = \frac{1}{4y} + \frac{\sqrt{Sb} A_c \sigma}{3} \frac{1}{kT} - \frac{1}{\sqrt{6}} (Sb)^{1/4} \sqrt{y} \ln S. \quad (29)$$

The procedure of Miller and Good involves transforming the original Schrödinger equation into a harmonic oscillator problem,

$$U''(S) + [\Gamma - S^2] U(S) = 0, \quad (30)$$

whose eigenvalues and eigenfunctions are  $\Gamma = \Gamma_n = 2n + 1$  and  $U(S) = U_n(S) = A_n H_n(S) e^{-S^2/2}$ , where the  $H_n(S)$  are the Hermite polynomials and the  $A_n$ 's are normalization constants. The Schrödinger eigenfunctions are then given by

$$\chi_n(y) = \frac{1}{\sqrt{S'(y)}} U[S(y)], \quad (31)$$

and the phase function  $S(y)$  is the solution of the first-order ordinary differential equation,

$$S'(y) = \left[ \frac{\lambda_n - V(y)}{\Gamma_n - S^2} \right]^{1/2}. \quad (32)$$

The requirement that  $S'(y)$  be finite at the turning points  $y_1$  and  $y_2$  gives the eigenvalue equation

$$\int_{-\sqrt{\Gamma}}^{\sqrt{\Gamma}} dS (\Gamma_n - S^2)^{1/2} = \int_{y_1}^{y_2} dy [\lambda_n - V(y)]^{1/2} = (n + \frac{1}{2})\pi. \quad (33)$$

The difficulty with the use of the Miller-Good approach is that it is applicable only when the boundary conditions are

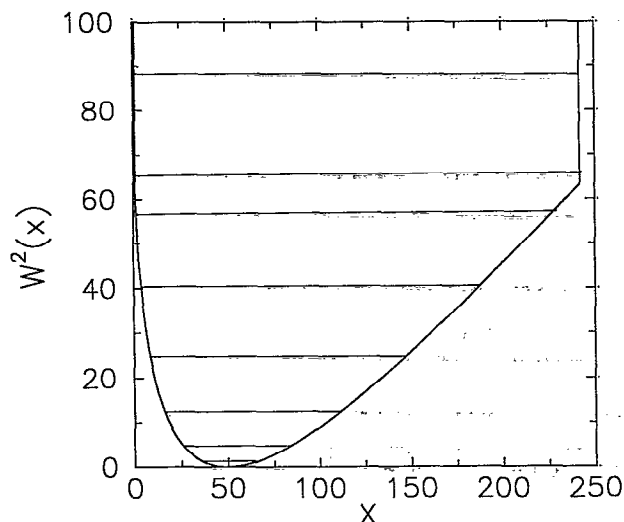


FIG. 1. Superpotential  $W^2(y(x))$  for  $N=242$  scaled by the factor  $q$ . The eigenvalues  $\lambda_n$  for  $n=1, 5, 10, 15, 25, 35, 40,$  and  $50$  are also shown.

the same as those of the harmonic oscillator, namely  $\chi_n(-\infty) = \chi_n(\infty) = 0$ , in which case both turning points are given by

$$\lambda_n - V(y) = 0. \quad (34)$$

In the present case, however, a different situation is encountered and the use of the uniform WKB theory of Miller and Good,<sup>12</sup> which has been successfully employed to the case of electron thermalization,<sup>14-16</sup> is more difficult. Because of the boundary conditions for Eq. (27), namely  $\chi_n(0) = \chi_n(y(N)) = 0$ , there appears to be three different types of eigenvalues with regard to the location of the turning points [assuming  $V(0) > V(y(N))$ ] as in I]: (i) eigenvalues  $\lambda_n < V(y(N))$ , for which both turning points are given by Eq. (34); (ii) eigenvalues  $V(y(N)) < \lambda_n < V(0)$ , for which  $y_1$  is given by Eq. (34) and  $y_2 = y(N)$ ; (iii) eigenvalues  $\lambda_n > V(0)$ , for which  $y_1 = 0$  and  $y_2 = y(N)$ . For

TABLE I. Eigenvalues  $\lambda_n$ .<sup>a</sup>

$n$	Exact	WKB	SWKB	% Dev WKB	% Dev SWKB
1	1.6349	1.6336	1.6349	-0.0766	-0.0008
5	8.1732	8.1718	8.1732	-0.0172	-0.0011
10	16.3433	16.3417	16.3432	-0.0100	-0.0012
15	24.5095	24.5077	24.5092	-0.0077	-0.0013
25	40.8265	40.8227	40.8246	-0.0092	-0.0047
35	57.2160	57.0967	57.0984	-0.2085	-0.2055
37	60.6055	60.3415	60.3428	-0.4357	-0.4334
40	66.0584	66.2313	65.4243	0.2617	-0.9599
50	88.3633	88.3895	87.5797	0.0296	-0.8869
55	101.7140	101.7280	100.9179	0.0138	-0.7827
60	116.4441	116.4517	115.6413	0.0065	-0.6894
65	132.5261	132.5294	131.7189	0.0025	-0.6091
70	149.9434	149.9436	149.1330	0.0002	-0.5404

<sup>a</sup>In  $\mu s^{-1}$  and with  $b=1$ .

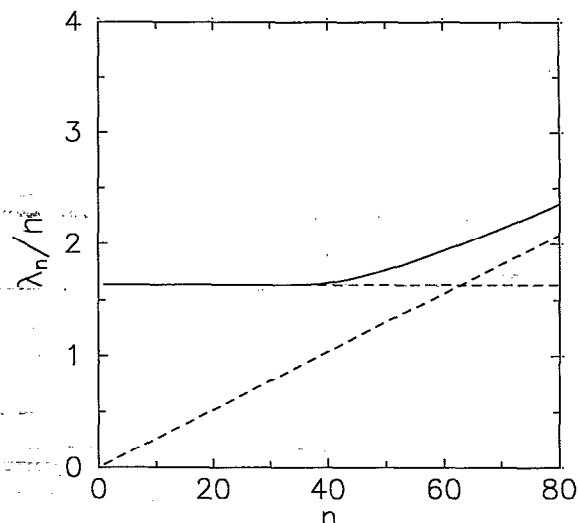


FIG. 2.  $\lambda_n$  vs  $n$  (solid line). The dashed lines represent the eigenvalues of the harmonic oscillator potential and of the square well.

the eigenvalues of type (iii), the traditional WKB method can be easily applied, giving the eigenfunctions

$$\psi_n(x) = \frac{1}{[B(x)]^{1/4}} \frac{1}{(\lambda_n - V)^{1/4}} \sin[S(y(x))], \quad (35)$$

with the phase function determined by

$$\begin{aligned} S(y(x)) &= \int_0^y dy [\lambda_n - V(y)]^{1/2} \\ &= \int_1^x \frac{dx}{\sqrt{B(x)}} [\lambda_n - V(y(x))]^{1/2}. \end{aligned} \quad (36)$$

The boundary condition at  $y=0$  is satisfied automatically, while the boundary condition at  $y(N)$  gives the eigenvalue equation

$$\begin{aligned} \int_0^{y(N)} dy [\lambda_n - V(y)]^{1/2} \\ = \int_1^N \frac{dx}{\sqrt{B(x)}} [\lambda_n - V(y(x))]^{1/2} = n\pi. \end{aligned} \quad (37)$$

For the eigenvalues of type (i), the Miller-Good procedure will give good approximations to the lower eigenfunctions, for which the second turning point is near the bottom of the potential. As  $y_2$  approaches  $y(N)$ , however, the eigenfunctions given by the Miller-Good method will not vanish at the upper boundary  $y(N)$  and the approximation will become worse for the eigenfunctions that correspond to the eigenvalues of type (ii). Since the maximum cluster size,  $x=N$ , is a free parameter of the theory, we can make use of it to improve the accuracy of the Miller-Good approximation to the eigenfunctions corresponding to eigenvalues of types (i) and (ii). In particular, it follows from the above discussion that if  $V(0) = V(y(N))$  there are no eigenvalues of type (ii) (for which the Miller-Good pro-

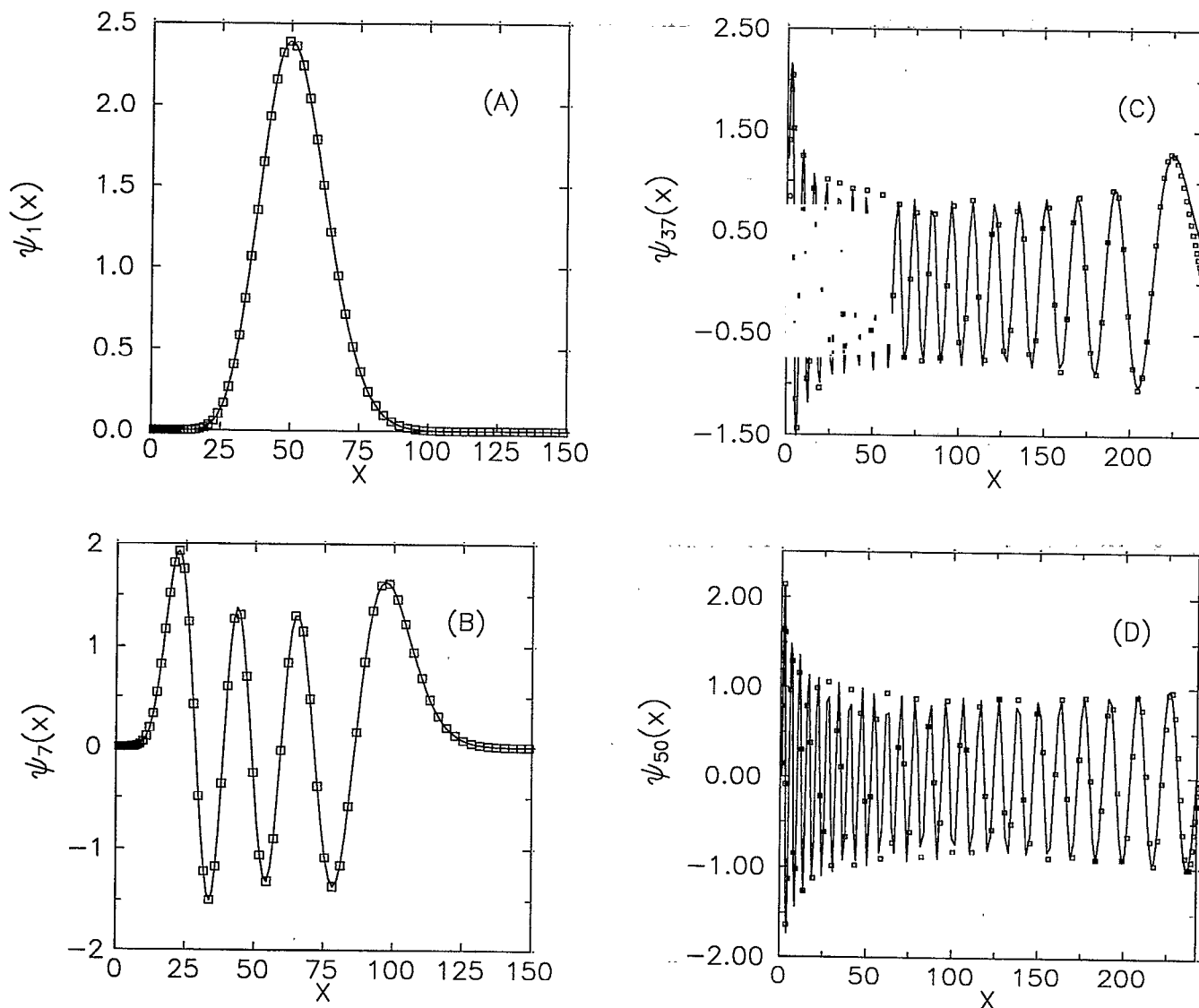


FIG. 3. Eigenfunctions  $\psi_n(x)$ . (A)  $n=1$ , (B)  $n=7$ , (C)  $n=37$ , (D)  $n=50$ . Solid line: WKB; squares: QDM.

cedure gives the worst approximation to the eigenfunctions) and this will be our criterion for choosing  $N$ .

### III. RESULTS AND DISCUSSION

In this section, we compare the WKB (and SWKB) solutions of the Fokker-Planck equation with the exact solution obtained with the quadrature discretization method (QDM) based on Legendre polynomials. The QDM method has been introduced and discussed elsewhere.<sup>17</sup> In our calculations, we will use the physical parameters typical of water at  $T=296$  K. We have  $A_c/kT = 11.81$ ,  $S=8.48$ , and  $b=3.6 \times 10^5 \text{ s}^{-1}$ . This gives  $x^* \approx 50$  and  $J^{\text{SS}} \approx 10 \text{ } 100 \text{ cm}^{-3}$ . With these values for the parameters, we have  $V(0) = V(y(N))$  for  $N=242$ .

In Fig. 1, we show the superpotential  $W^2$ , scaled by the factor

$$q = \frac{2 A_c \sigma}{9 kT} S b (x^*)^{-2/3}, \quad (38)$$

as a function of  $x$ , and in Table I we show the WKB and SWKB approximations to some of the eigenvalues, scaled by the factor  $b$ , together with the exact ones and the percentage errors. The horizontal lines in Fig. 1 are the eigenvalues  $\lambda_n$ ,  $n=1, 5, 10, 15, 25, 35, 40, 50$ . Here and in all the examples that follow we have used  $x_0=15$ . The minimum of the potential occurs near  $x^*$  and  $V(y)$  is well approximated by a quadratic near the minimum, that is,  $V(y)$  is very close to the potential of the harmonic oscillator. For the eigenvalues  $\lambda_n$ ,  $n \leq 38$ , the turning points occur within the interval  $[1, N]$  while for all the higher eigenvalues the turning points are  $x=1$  and  $x=N$ . As we see in Table I, the agreement between the WKB and SWKB eigenvalues and the exact ones is excellent.

In Fig. 2 we show the ratio  $\lambda_n/n$  vs  $n$ . The lowest eigenvalues, up to  $n \approx 40$ , are proportional to  $n$ , as for the

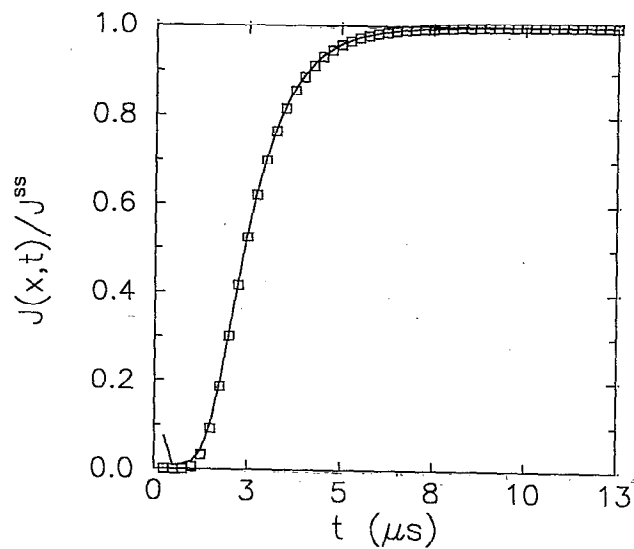


FIG. 4. Ratio  $J(x,t)/J^{ss}$  vs  $t$  at  $x \approx 50.6$ . Solid line: WKB; squares: QDM.

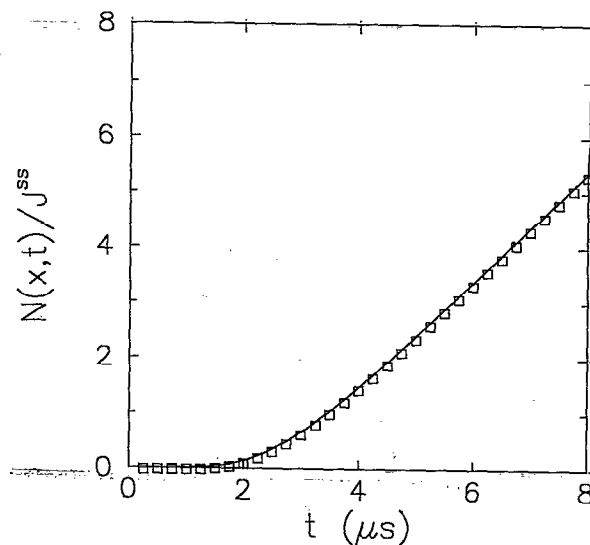


FIG. 5. Ratio  $N(x,t)/J^{ss}$  vs  $t$  at  $x \approx 50.6$ . Solid line: WKB; squares: QDM.

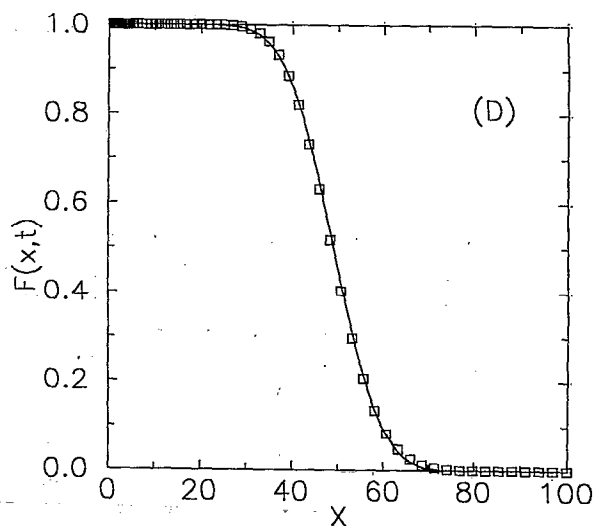
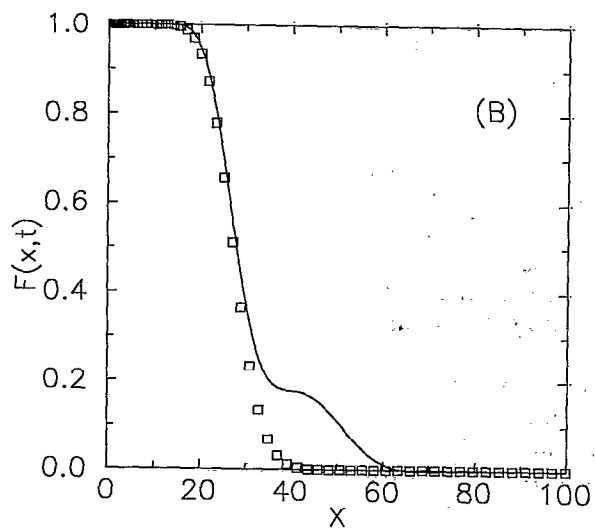
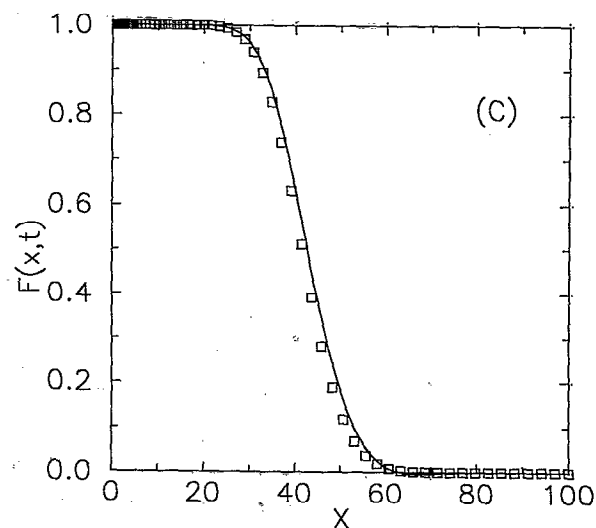
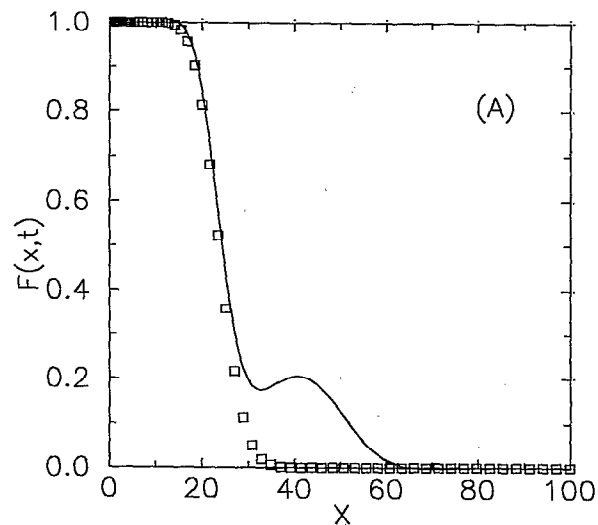


FIG. 6. Distribution function  $F(x,t)$  at (A)  $t=0.5 \mu s$ , (B)  $t=0.75 \mu s$ , (C)  $t=2.5 \mu s$ , and (D)  $t=6 \mu s$ . Solid line: WKB; squares: QDM.

eigenvalues of the harmonic oscillator. At very high  $n$ , the eigenvalues are proportional to  $n^2$ , as for the eigenvalues of a square well. The horizontal dashed line corresponds to the harmonic oscillator eigenvalues and the linear dashed line is for the square well eigenvalues.

In Figs. 3(A)–3(D) we compare the WKB approximation for some of the eigenfunctions with the exact ones. The agreement is excellent for all eigenfunctions, except for small discrepancies for  $30 \leq n \leq 40$ .

Figure 4 shows the nucleation flux  $J(x,t)/J^{\text{SS}}$  for  $x \approx 50.6$  (recall that  $x^* = 50$ ) as a function of time. The approach to the steady state is described accurately and the agreement is excellent at all times except near  $t \approx 0$ . As discussed in Ref. 16, this is due to the fact that an exact discrete completeness relation for the WKB eigenfunctions does not hold, while for the QDM eigenfunctions we have that  $\sum_{n=0}^N \omega_n \phi_n(x_i) \phi_n(x_j) = \delta_{ij}$  (here, the  $\{x_i\}_{i=0}^N$  are the Legendre quadrature points), which guarantees the exact fitting of the initial condition. Because of the inaccurate values of the WKB approximation to the nucleation flux at short times, the WKB result for the integrated flux  $N(x,t)/J^{\text{SS}}$  differs from the exact one by a constant term. In Fig. 5 we show  $N(x,t)/J^{\text{SS}}$  (also for  $x \approx 50.6$ ) as a function of time, after the spurious constant has been subtracted out. The time lag predicted by the WKB method,  $\tau = 2.645 \mu\text{s}$ , is in good agreement with the exact value  $\tau = 2.714 \mu\text{s}$ .

In Figs. 6(A)–6(D) we show the distribution function  $F(x,t)$  at four different times,  $t = 0.5, 0.75, 2.5,$  and  $6 \mu\text{s}$ . For times  $t \approx 2.5 \mu\text{s}$  and larger, the WKB and the exact solutions are in good agreement. The discrepancy at short times, which we have already seen in the fluxes, appears here in the tail of the distribution, where the WKB solution develops a bump, not present in the exact cluster distribution. By  $t \approx 2.5 \mu\text{s}$  the bump has disappeared.

#### IV. CONCLUSIONS

In this work, we have shown how the WKB and SWKB methods can be used to find approximate solutions of the Fokker–Planck-type equations that arise in homogeneous nucleation theory. The Fokker–Planck equation is transformed into a Schrödinger eigenvalue problem with

an appropriate potential and the WKB and SWKB methods are employed to determine the eigenvalues and eigenfunctions. The agreement of the WKB and SWKB eigenvalues and eigenfunctions with the exact ones is generally very good. The Schrödinger potential for the nucleation problem is well approximated by the harmonic oscillator potential near the critical cluster size (coinciding with the minimum of the potential) while it is close to a square well near the boundaries. This is confirmed by the behavior of the eigenvalues, the lower ones being proportional to  $n$  and the higher ones being proportional to  $n^2$ . The WKB approximation to the cluster distribution function and to the nucleation flux is good at moderately large times, when the fast transients described by the higher eigenvalues (and eigenfunctions) have died out. The discrepancies that we have seen at short times, which are due to the lack of exact discrete orthogonality and completeness relations for the WKB eigenfunctions, are small and the approach to the steady state is described accurately. In particular, the WKB method gives accurate values for the time lags.

#### ACKNOWLEDGMENTS

This research is supported by a grant from the Natural Sciences and Engineering Research Council of Canada, and an Atmospheric Environment Science subvention.

- <sup>1</sup>R. Becker and W. Döring, *Ann. Phys. (N.Y.)* **24**, 719 (1935).
- <sup>2</sup>J. Frenkel, *Kinetic Theory of Liquids* (Oxford University Press, Oxford, 1946).
- <sup>3</sup>F. C. Goodrich, *Proc. R. Soc. London, Ser. A* **277**, 167 (1964).
- <sup>4</sup>B. Shizgal and J. C. Barrett, *J. Chem. Phys.* **91**, 6505 (1989).
- <sup>5</sup>D. T. Wu, *J. Chem. Phys.* **97**, 1922 (1992); **97**, 2644 (1992).
- <sup>6</sup>D. Kashiev, *Surf. Sci.* **14**, 209 (1969).
- <sup>7</sup>K. Binder and D. Stauffer, *Adv. Phys.* **25**, 343 (1976).
- <sup>8</sup>H. Trinkaus and M. H. Yoo, *Philos. Mag.* **55**, 269 (1987).
- <sup>9</sup>J. Edrei and M. Gitterman, *Phys. Rev. A* **33**, 2821 (1986).
- <sup>10</sup>Y. Rabin and M. Gitterman, *Phys. Rev. A* **29**, 1496 (1984).
- <sup>11</sup>G. Shi, J. H. Seinfeld, and K. Okuyama, *Phys. Rev. A* **41**, 2101 (1990).
- <sup>12</sup>S. C. Miller and R. H. Good, *Phys. Rev.* **91**, 174 (1953).
- <sup>13</sup>S. H. Fricke, A. B. Balentkin, P. J. Hatchell, and T. Uzer, *Phys. Rev. A* **37**, 2797 (1988).
- <sup>14</sup>B. Shizgal and T. Nishigori, *Chem. Phys. Lett.* **171**, 493 (1990).
- <sup>15</sup>B. Shizgal, *Can. J. Phys.* **68**, 1213 (1990).
- <sup>16</sup>B. Shizgal and L. Demeio, *Can. J. Phys.* **69**, 712 (1991).
- <sup>17</sup>R. Blackmore and B. Shizgal, *J. Chem. Phys.* **31**, 1855 (1985); B. Shizgal and D. R. A. McMahon, *ibid.* **32**, 3669 (1985); B. Shizgal and R. Blackmore, *J. Comput. Phys.* **55**, 31 (1984).